



HAL
open science

Flow birefringence study at the transition from laminar to Taylor vortex flow

J.P. Decruppe, R. Hocquart, T. Wydro, R. Cressely

► **To cite this version:**

J.P. Decruppe, R. Hocquart, T. Wydro, R. Cressely. Flow birefringence study at the transition from laminar to Taylor vortex flow. *Journal de Physique*, 1989, 50 (23), pp.3371-3394. 10.1051/jphys:0198900500230337100 . jpa-00211149

HAL Id: jpa-00211149

<https://hal.science/jpa-00211149>

Submitted on 4 Feb 2008

HAL is a multi-disciplinary open access archive for the deposit and dissemination of scientific research documents, whether they are published or not. The documents may come from teaching and research institutions in France or abroad, or from public or private research centers.

L'archive ouverte pluridisciplinaire **HAL**, est destinée au dépôt et à la diffusion de documents scientifiques de niveau recherche, publiés ou non, émanant des établissements d'enseignement et de recherche français ou étrangers, des laboratoires publics ou privés.

LE JOURNAL DE PHYSIQUE

J. Phys. France 50 (1989) 3371-3394

1^{er} DÉCEMBRE 1989, PAGE 3371

Classification
Physics Abstracts
78.20Fm

Flow birefringence study at the transition from laminar to Taylor vortex flow

J. P. Decruppe, R. Hocquart, T. Wydro and R. Cressely

Laboratoire de Physique des Polymères, Faculté des Sciences, Ile du Saulcy, 57000 Metz, France
(Reçu le 16 janvier 1989, révisé le 20 juillet 1989, accepté le 24 août 1989)

Résumé. — La biréfringence induite par l'écoulement dans un liquide contenant de fines particules et confiné entre deux cylindres coaxiaux est étudiée au voisinage de la transition entre écoulement de Couette et tourbillons de Taylor. Après avoir établi l'expression analytique du champ hydrodynamique dans le domaine d'écoulement axisymétrique, nous en déduisons la vitesse angulaire d'une particule entraînée par ce champ puis la fonction de distribution des orientations de la particule. Moyennant certaines hypothèses simplificatrices mais néanmoins réalistes, on montre que les expressions théoriques de l'angle d'extinction χ et de l'intensité de la biréfringence induite Δn s'obtiennent en considérant la suspension comme une superposition de couches infiniment minces d'orientation continuellement variable. Les résultats théoriques sont ensuite comparés aux courbes expérimentales tracées à l'aide de mesures effectuées sur des suspensions de deux types de particules : la bentonite et le virus de la mosaïque du tabac. En écoulement de Couette, la forme des particules en solution n'influe pas sur l'allure générale des courbes $\chi(G)$ et $\Delta n(G)$, G étant le gradient de cisaillement dans l'espace annulaire. Il n'en est plus de même en écoulement axisymétrique de Taylor pour lequel ces mêmes courbes présentent un aspect différent pour les solutions contenant des particules allongées (V.M.T.) ou aplaties (bentonite). Ces résultats sont confirmés par le calcul théorique.

Abstract. — We have studied the birefringence induced by the flow in a liquid containing very fine particles in the vicinity of the transition between the Couette flow and the Taylor vortex flow. We derive at first an analytical expression of the axisymmetrical hydrodynamical field and then the angular velocity of a particle in the flow. The resolution of the diffusion equation leads to the orientation distribution function F . On condition of some simplifying but realistic hypotheses, we show that the extinction angle χ and the birefringence Δn of the solution are the same as the properties of an equivalent stratified medium composed of very thin layers the orientation of which varies continuously. The results concerning the velocity profile and the critical Taylor number are in good agreement with other sources ; the theoretical computation of χ and Δn are then compared to experimental curves realized with solutions of bentonite and T.M.V. ; interesting conclusions can be drawn on the influence of the shape of the particles on the behavior of the angle of extinction and of the birefringence intensity in the region of the Taylor vortex flow.

1. Introduction.

In his original theoretical and experimental work Taylor [1] showed that when the angular velocity of the inner rotating cylinder of a conventional Couette cell reaches a critical value

depending on the geometry of the cell, the velocity profile in the gap between the cylinders changes suddenly, giving rise to the well-known three dimensional and stable flow called Taylor vortex flow.

Now, if we are interested in the flow of diluted solutions of rigid particles, the average orientation of a particle at the different points of the annular gap when the vortex flow is established, will undoubtedly differ from the orientation it will have in a conventional Couette flow. If, in addition the medium presents flow birefringence, it is then not surprising to notice an important change in the behaviour of the angle of extinction χ and of the birefringence intensity Δn as a function of the velocity gradient when the critical value is reached.

Previous work [2] and more recent experiments [3] performed on solutions of clay materials show clearly this assumption.

Adequate theoretical interpretation of these curves have been developed in the past [4-8] for the Couette flow but concerning the Taylor vortex flow no theoretical studies of these optical properties have been done.

The aim of this paper is to work out the theoretical expressions for the birefringence intensity Δn and for the extinction angle χ of suspensions of rigid particles undergoing the axisymmetrical Taylor flow.

The comparison between theoretical predictions and experimental measurements performed on solutions of clay material and Tobacco mosaic virus (TMV) seems to confirm the validity of the model derived from the linearized Navier-Stokes equations and allow interesting conclusions about the effect of the shape of the particles on the behaviour of χ and Δn at the transition.

2. Theoretical.

In order to calculate the birefringence intensity, which characterizes the degree of orientation of the particles and the extinction angle defined as the angle between the line of flow and a neutral line of the liquid, we ought to know the orientation distribution function F of the particle, function which depends itself on the hydrodynamical field in the cell.

The main difficulty of the above mentioned problem lies in the determination of the function F . If, for instance, we consider an orthotropic body, there is no coupling between translational and rotational motion and F satisfies the rotational diffusion equation [9] :

$$\frac{\partial F}{\partial t} + \nabla \cdot (F\omega) = 0$$

where the operator $\nabla = \sum_1^3 \mathbf{e}_i \frac{\partial}{\partial \alpha_i}$; \mathbf{e}_i is the unit vector along the principal axis i , α_i the rotation about this axis and ω stands for the angular velocity.

If, in addition, the particle is of revolution, the rotation about the axis of revolution has no physical meaning. Let \mathbf{u} be the unit vector along this axis, the diffusion equation becomes :

$$\frac{\partial F}{\partial t} + \mathfrak{R} \cdot (\omega F) = 0$$

in which $\nabla \equiv \mathfrak{R} = \mathbf{u} \wedge \frac{\partial}{\partial \mathbf{u}}$ is the well-known rotational operator. (In quantum mechanics, $-j\mathfrak{R}$ corresponds to the angular momentum operator). The previous equation may also be written as :

$$\frac{\partial F}{\partial t} + \mathfrak{R} \cdot (\omega F) = \frac{\partial F}{\partial t} + \frac{\partial}{\partial \mathbf{u}} \cdot (\omega \wedge \mathbf{u} F) = \frac{\partial F}{\partial t} + \frac{\partial}{\partial \mathbf{u}} \cdot (\dot{\mathbf{u}} F) = 0$$

$\dot{\mathbf{u}}$ is the time derivative of the orientation vector \mathbf{u} .

The angular velocity ω or the vector \mathbf{u} can be expressed as follow :

$$\omega = \omega_B + \omega_H ; \quad \dot{\mathbf{u}} = \dot{\mathbf{u}}_B + \dot{\mathbf{u}}_H .$$

The first and second term in the right hand side represent respectively the Brownian contribution and the hydrodynamic part to the rotational velocity of the particle. While the first one depends on the geometrical form on the particle, the second one requires the knowledge of the hydrodynamical field in the gap of the Couette cell.

Concerning the optical part of the problem, the study of the polarization of the medium under the action of the electrical field of the incident light will lead to the principal permittivities of the medium from which we shall merely deduce Δn and χ .

2.1 HYDRODYNAMICAL FIELD. — Let us follow the method of Chandrasekar [10] to find a solution of the linearized Navier-Stokes equations and assume that the three dimensional flow results from the superposition of a small axisymmetric perturbation to the laminar flow.

Calling u_r, u_θ, u_z the three components of the perturbation in the steady state, we write :

$$\begin{aligned} u_r &= u(r) \cos kz \\ u_\theta &= v(r) \cos kz \\ u_z &= w(r) \sin kz \end{aligned}$$

we get, after some handling of the N.S. and continuity equations, the well-known sixth-order differential equation relating $v(x)$ and its derivatives.

$$(D^2 - a^2)^3 v(x) = - Ta^2(1 + \xi x) v(x) \tag{2.1}$$

together with the boundary conditions :

$$v(x) = (D^2 - a^2) v(x) = D(D^2 - a^2) v(x) = 0 \quad \text{for } x = 0 \quad \text{and } 1$$

x stands for a dimensionless variable related to r by

$$x = (r - R_1)/d$$

the operator $D = \frac{d}{dx}$, $a = k/d$ and $\xi = - \left(1 - \frac{\Omega_2}{\Omega_1} \right)$;

R_1 and d being respectively the radius of the inner cylinder and the width of the annular gap, T is the classical Taylor number and Ω_1, Ω_2 respectively the angular velocity of the inner and outer cylinder.

It should be made clear that equation (2.1) holds only in the small gap approximation (width of the annular gap smaller than the radii of the cylinders). Since only the inner cylinder is rotating, ξ will be set to $- 1$.

Although the exact solutions of equation (2.1) are known [11, 12], they appear as an integral representation which does not allow for an easy handling in further developments ; thereby we shall seek for a simpler approximated expression.

Integrating equation (2.1) leads to a Volterra equation :

$$v(x) = v_0(x) - \frac{T}{8 a^3} \int_0^x F(x, t)(x - t) v(t) dt$$

where $F(x, t) = a^2(x - t)^2 \text{sh } a(x - t) - 3 a(x - t) \text{ch } a(x - t) + 3 \text{sh } a(x - t)$.

A solution of this latest equation is written as :

$$v(x) = \sum_{i=0}^{\infty} (-1)^i \left[\frac{T}{8a^3} \right]^i v_i(x)$$

where the different $v_i(x)$ satisfy :

$$v_i(x) = \int_0^x F(x, t)(x-t) v_{i-1}(t) dt .$$

The approximation of order zero to the solution $v_0(x)$ is readily evaluated and is expressed as :

$$v_0(x) = A \operatorname{sh} ax + B (ax^2 \operatorname{ch} ax - x \operatorname{sh} ax) + C (ax^2 \operatorname{sh} ax - 3x \operatorname{ch} ax)$$

expression which satisfies the three boundary conditions for $x = 0$.

The constants A , B , C are related to the first, fourth and fifth derivatives of $v(x)$ calculated for $x = 0$.

Generally speaking a term $v_i(x)$ will write as :

$$v_i(x) = Av_{A,i}(x) + Bv_{B,i}(x) + Cv_{C,i}(x) .$$

The number of such factors in the expression of $v(x)$ is determined in the following way : let the boundary conditions be applied for $x = 1$ to the three components $u(x)$, $v(x)$, $w(x)$ of the perturbation ; we get an homogeneous system of three equations with the constants A , B , and C as unknowns and T and a as parameters. For different values of a , we seek for a solution of the system by allowing T to vary until the determinant of the coefficients equals zero. Among all the values chosen for a , one of them leads to a minimum for T which is then the Taylor number we are looking for.

Satisfactory results have been obtained by including terms up to the second approximation in $v(x)$ and we found for a and T values which are in excellent agreement with different authors as can be seen in table I.

The radial part of the three components can be written for :

— the tangential component

$$v(x) = v_0(x) - \frac{T}{8a^3} [Av_{A,i}(x) + Bv_{B,i}(x) + Cv_{C,i}(x)] + \left[\frac{T}{8a^3} \right]^2 [Av_{A,2}(x) + Bv_{B,2}(x) + Cv_{C,i}(x)]$$

— the radial component

$$u(x) = \frac{\nu}{2Ad^2} (D^2 - a^2) v(x)$$

with ν standing for the viscosity of solution ;

— the axial component

$$w(x) = -\frac{1}{a} Du(x) .$$

Table I. — *Critical Taylor numbers obtained through different methods.*

Authors	Paramètre <i>a</i>	First approximation	Second approximation	Third approximation
Our results	3.12	2 539	3 394.3	3 389.9
Chandrasekar [9]	3.12	3 429.9	3 406.9	3 390.3
Nsom [11]	3.12	Direct computation of the solution 3 389		
Davey [12]	3.12	Numerical resolution of the equations 3 389.9		
Krueger et Co. [20]	3.12	Numerical resolution of the equations 3 390.1		
Eagles [21]	3.127	Velocity expanded as a series 3 390		

Table II compares the relative values of the different components with other authors. These former equations can be used to compute the components of the perturbation in the approximation of a small gap and as long as the flow remains in its first stage (no azimuthal

Table II. — *Components of the perturbation at the transition from Couette flow to Taylor vortex flow.*

Position in the annular gap	Tangential component : <i>v</i>			Radial component : <i>u</i>		Axial component : <i>w</i>
	our results	[12] Davey	[11] Nsom	our results	[12] Davey	our results
0	0	0	0	0.000	0	0
0.1	0.287	0.288	0.288	0.151	0.151	− 0.802
0.2	0.568	0.569	0.568	0.461	0.463	− 1
0.3	0.805	0.806	0.808	0.764	0.767	− 0.791
0.4	0.957	0.958	0.957	0.957	0.960	− 0.360
0.48	1.000			1		
0.5	0.999	1.000	0.999	0.994	0.998	+ 0.133
0.6	0.926	0.927	0.926	0.877	0.881	0.559
0.7	0.756	0.758	0.757	0.644	0.647	0.824
0.8	0.523	0.524	0.523	0.360	0.362	0.858
0.9	0.261	0.262	0.262	0.111	0.117	0.608
1	0	0	0.000	0	0	0

wave). However it should be noticed that neither this method of resolution nor the study of the growth of the vortices [13] lead to an absolute value of the three components of the velocity field.

Following Davey [13] who showed that the equilibrium amplitude A_e of the motion obeys to the law :

$$A_e \propto \left(1 - \frac{T_c}{T}\right)^{1/2}$$

relative value of $v(x)$, $u(x)$ and $w(x)$ can be evaluated once T and a have been determined.

However, a look at the marginal stability curve (Fig. 1) shows that, for each $T > T_c$, two values of a ($a = k/d$) are equally possible and as far as T remains in the direct vicinity of T_c , there is no experimental nor theoretical evidence to choose the smaller rather than the greater value of a .

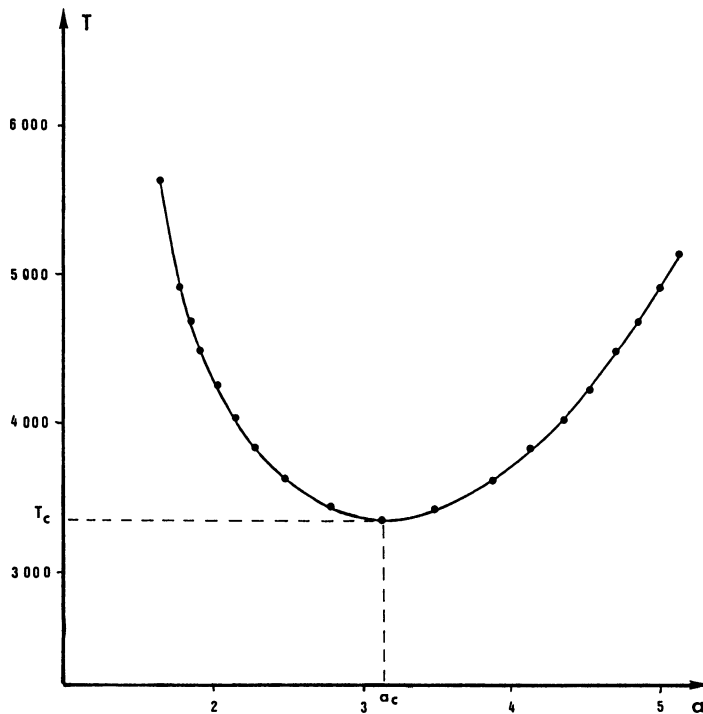


Fig. 1. — Marginal stability curve.

The figures 2-7 represent respectively the relative variations, as a function of x , of the tangential, radial and axial component of the perturbation for both cases $a < a_c$ and $a > a_c$ and for different values of the Taylor number T . In each set, the curves are ordered according to ascending values of T : the curve with the smallest maximum corresponding to the smallest value of the Taylor number. These values of T are chosen so that the corresponding shear rates are identical to those used in the experiments and are :

Table III. — Taylor numbers and values of a used in the curves 2-7.

Shear rate (s^{-1})	Taylor number	a ($a < a_c$)	a ($a > a_c$)
35.9	3 456.8	2.83	3.42
36.8	3 617.2	2.50	3.82
38.1	3 877.0	2.26	4.17
40.6	4 410.0	1.96	4.66
43.2	4 981.2	1.76	5.03
45.7	5 583.0	1.61	5.34
48.3	6 221.0	1.48	5.58

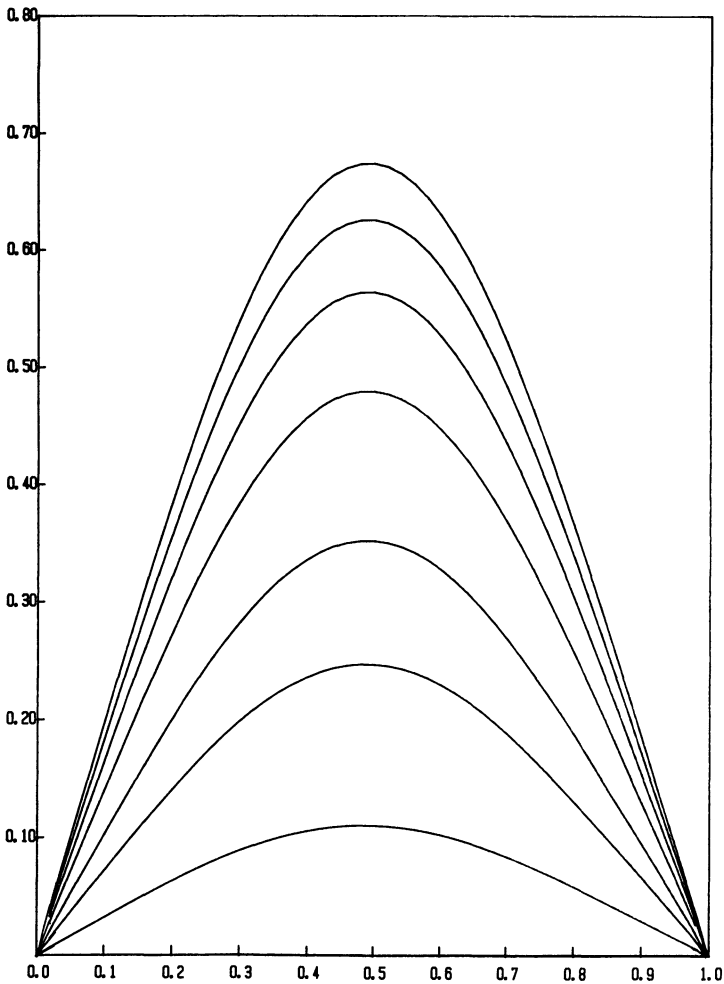


Fig. 2. — Tangential component of the perturbation for different values of the Taylor number in the case $a < a_c$ (Taylor number and values of a listed in Tab. III).

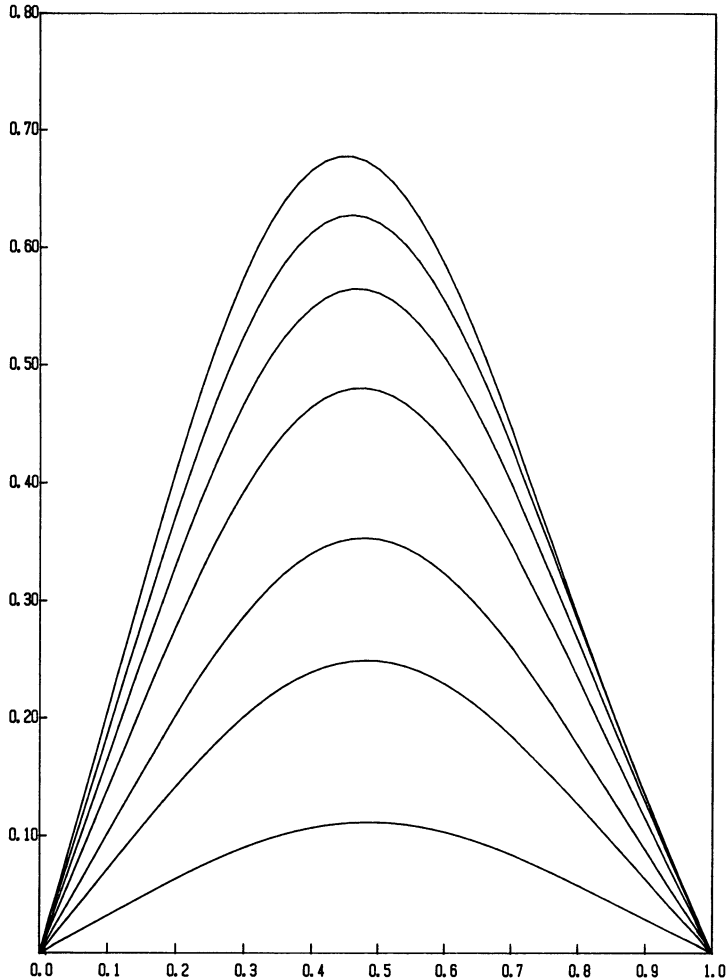


Fig. 3. — Tangential component of the perturbation for different values of the Taylor number in the case $a > a_c$ (Taylor number and values of a listed in Tab. III).

For a given a , the tangential component v of the perturbation appears to be the principal one being roughly ten times more important than the others. For a given T , the values of this same component v appear to be very similar for a greater or smaller than a_c .

Concerning the radial component $u(x)$, there is a significant difference between the maxima of the different curves corresponding to the cases ($a >$ or $< a_c$): the highest values for a given G (shear rate $\frac{\Omega_1 R_1}{d}$) being obtained in the case $a > a_c$; as G is increased and reaches the final value, the radial component tends not to increase any more when $a < a_c$; this conclusion does not hold for the other case $a > a_c$.

However, in any case we ought to remember that these curves represent only relative variations since a multiplicative factor remains in the equations.

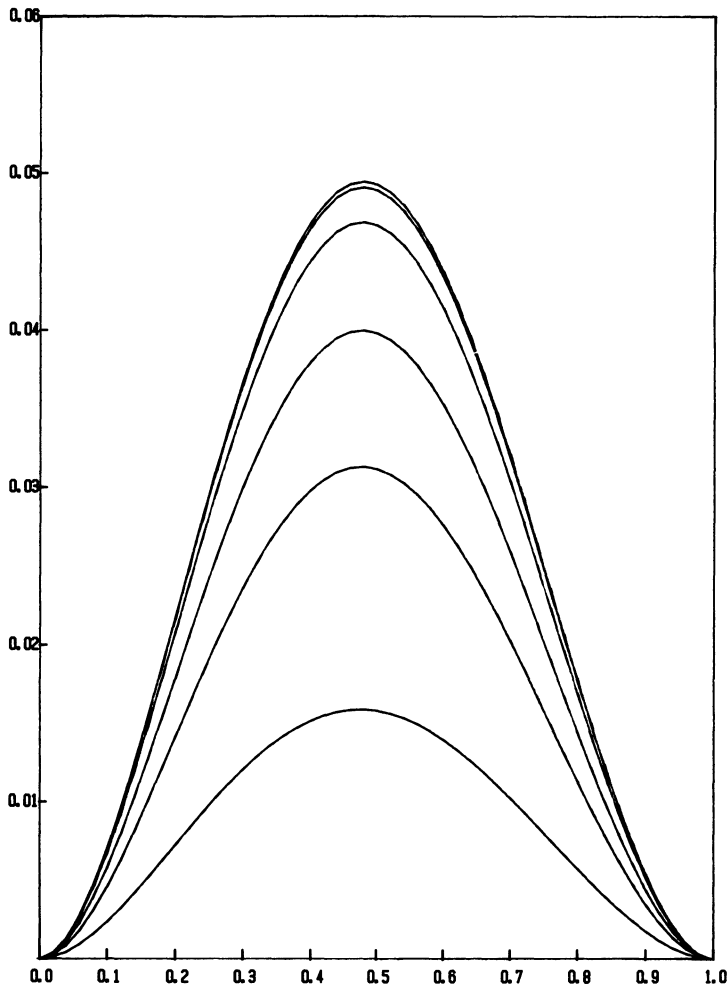


Fig. 4. — Radial component of the perturbation for different values of the Taylor number in the case $a < a_c$ (Taylor number and values of a listed in Tab. III).

2.2 STATISTICAL ORIENTATION OF THE PARTICLES. — Suppose now that the liquid contains small particles carried away by the flow ; under the combined but antagonist action of the Brownian motion and of the hydrodynamical field, the particles will take a preferred orientation in the direction (θ, φ) (see Fig. 8) characterised by the orientation distribution function $F(\theta, \varphi)$ which satisfies :

$$\mathfrak{R} \cdot (F(\boldsymbol{\omega}_H + \boldsymbol{\omega}_B)) = \frac{\partial}{\partial \mathbf{u}} \cdot (F(\dot{\mathbf{u}}_H + \dot{\mathbf{u}}_B)) = 0 . \tag{2.2}$$

2.2.1 *Brownian velocity.* — For a prolate or oblate spheroidal particle, $\boldsymbol{\omega}_B$ is given by the relation :

$$\boldsymbol{\omega}_B = -D_r \mathfrak{R} \text{Log } F = -D_r \left[\frac{1}{F} \frac{\partial F}{\partial \theta} \mathbf{e}_\varphi - \frac{1}{F \sin \theta} \frac{\partial F}{\partial \varphi} \mathbf{e}_\theta \right]$$

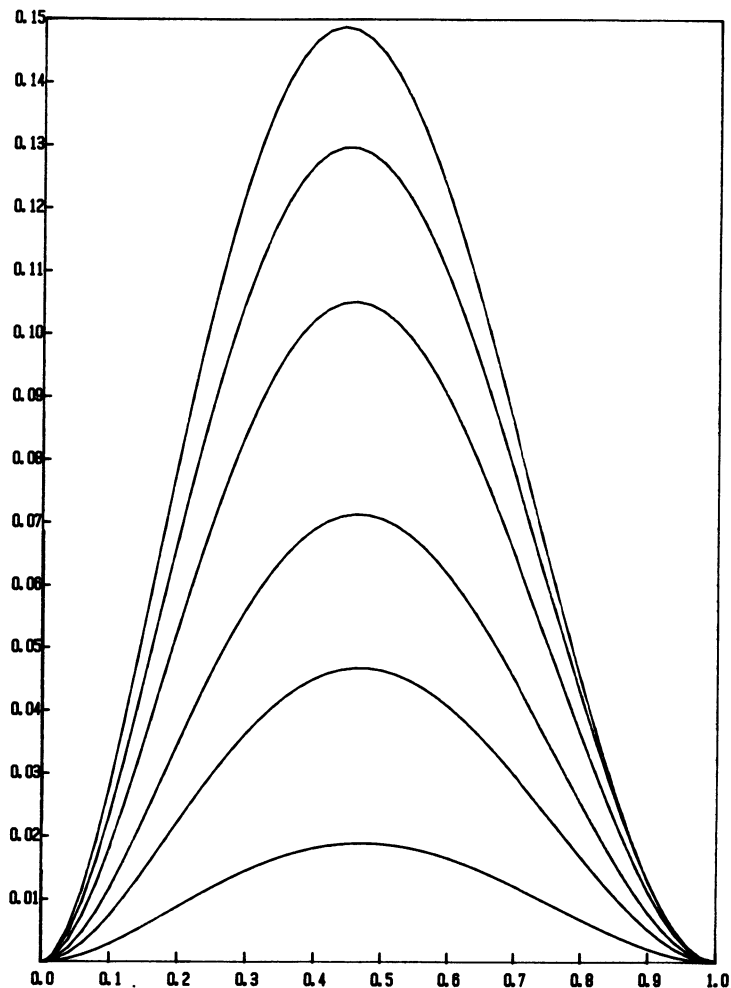


Fig. 5. — Radial component of the perturbation for different values of the Taylor number in the case $a > a_c$ (Taylor number and values of a listed in Tab. III).

where D_r is the rotational diffusion coefficient around a transverse axis of the particle and $\mathbf{e}_\theta, \mathbf{e}_\varphi$, the unit vectors in the θ and φ directions.

In the same way, we have :

$$\dot{\mathbf{u}}_B = -D_r \frac{\partial F}{\partial \mathbf{u}} = -D_r \left[\frac{1}{F} \frac{\partial F}{\partial \theta} \mathbf{e}_\theta + \frac{1}{F \sin \theta} \frac{\partial F}{\partial \varphi} \mathbf{e}_\varphi \right].$$

2.2.2 Hydrodynamic velocity. — This calculation is based upon the following hypotheses : the velocity of the particle equals that of the fluid (no slip condition) and its variations are instantaneous ; in addition, we will suppose that the centre of gravity of the particle moves with the velocity of the liquid at this point.

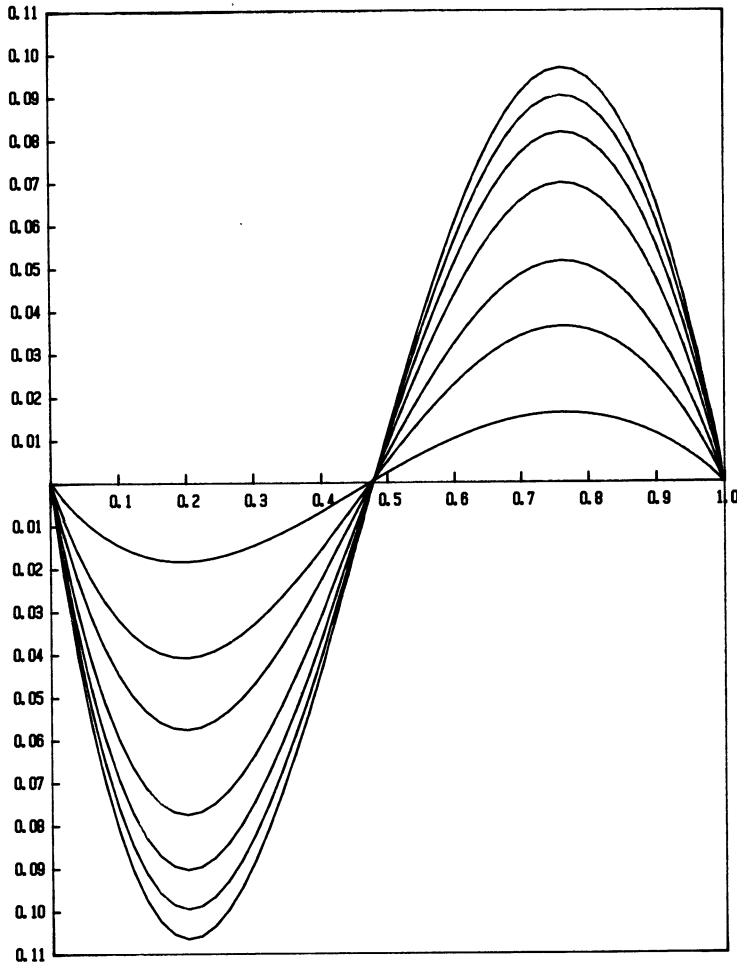


Fig. 6. — Axial component of the perturbation for different values of the Taylor number in the case $a < a_c$ (Taylor number and values of a listed in Tab. III).

Taking into account Jeffery's work [14] concerning the Couette flow, the two components of the spin of the particle assumed to be a spheroid, are :

$$\begin{aligned} \dot{\theta} = & \frac{b}{4d} \sin(2\varphi) \sin(2\theta) \left[-\Omega_1 R_1 + \frac{\partial v(x)}{\partial x} \cos(kz) \right] \\ & + k \cos \varphi \left[\frac{1}{2}(b-1) - \cos^2 \theta \right] u(x) \sin(kz) \\ & + k \sin \varphi \left[\frac{1}{2}(b-1) - \cos^2 \theta \right] v(x) \sin(kz) \\ & + \frac{\cos \varphi}{d} \left[\frac{1}{2}(b-1) - b \sin^2 \theta \right] \frac{\partial w(x)}{\partial x} \sin(kz) \\ & + \frac{b}{4d} \cos(2\varphi) \sin(2\theta) \frac{\partial u(x)}{\partial x} \cos(kz) - \frac{3}{4} bkw(x) \sin(2\theta) \cos(kz) \end{aligned}$$

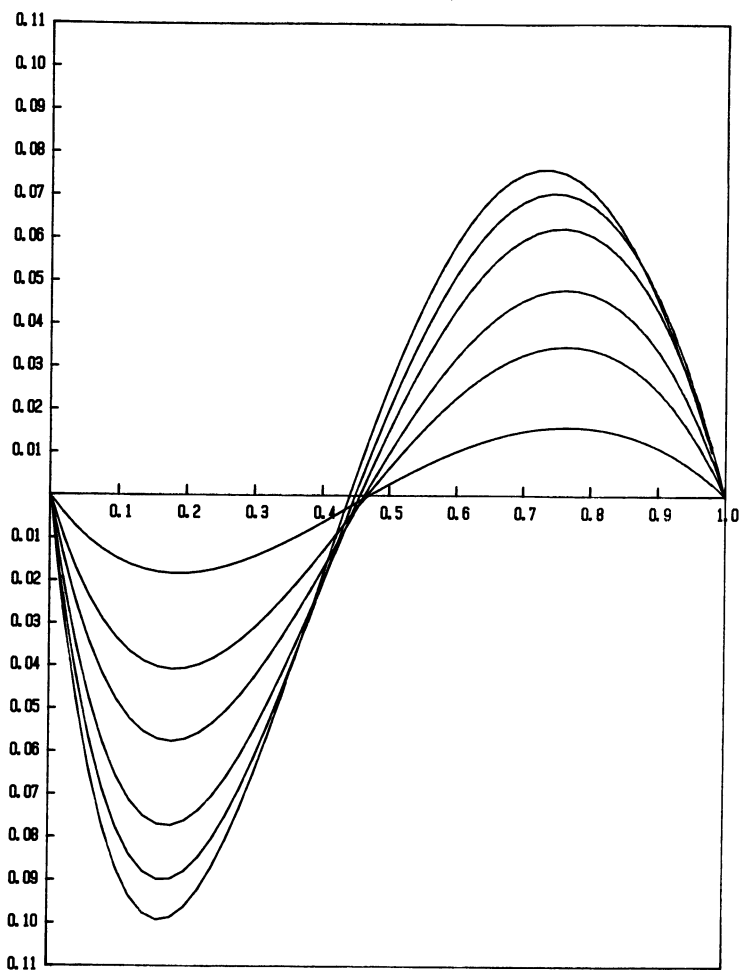


Fig. 7. — Axial component of the perturbation for different values of the Taylor number in the case $a > a_c$ (Taylor number and values of a listed in Tab. III).

$$\begin{aligned} \dot{\varphi} = & \frac{1}{2d} [b \cos(2\varphi) + 1] \left[-\Omega_1 R_1 + \frac{\partial v(x)}{\partial x} \cos(kz) \right] \\ & + \frac{k}{2} \cotg \theta \sin \varphi (b+1) u(x) \sin(kz) - \frac{b}{2d} \sin(2\varphi) \frac{\partial u(x)}{\partial x} \cos(kz) \\ & + \frac{k}{2} \cotg \theta \cos \varphi (b-1) v(x) \sin(kz) + \frac{1}{2d} \cotg \theta (1-b) \sin(\varphi) \frac{\partial w(x)}{\partial x} \sin(kz) \end{aligned}$$

where b is the shape factor of the particle defined as the ratio $\frac{p^2-1}{p^2+1}$; p stands for the ratio of the axes of the spheroid.

Once, we know $\dot{\theta}$ and $\dot{\varphi}$, it is easy to get ω_H or $\dot{\mathbf{u}}_H$ since :

$$\omega_H = \dot{\theta} \mathbf{e}_\varphi - \dot{\varphi} \sin \theta \mathbf{e}_\theta ; \quad \dot{\mathbf{u}}_H = \dot{\theta} \mathbf{e}_\theta + \dot{\varphi} \sin \theta \mathbf{e}_\varphi .$$

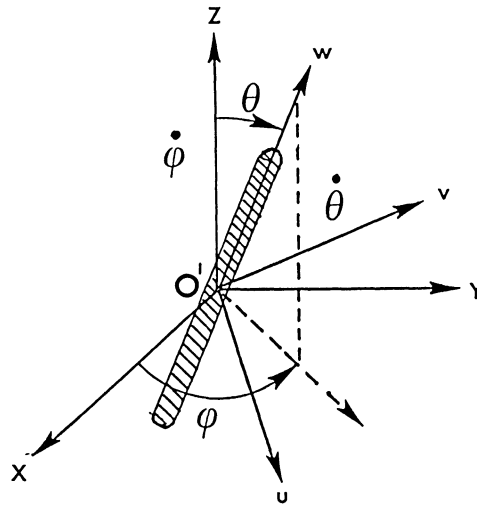


Fig. 8. — Coordinates system and orientation of a particle.

2.2.3 Diffusion equation and mathematical expression of F . — Introducing the expressions of ω_B and ω_H in equation (2.2) we obtain :

$$D_r \Delta F = \frac{1}{\sin \theta} \frac{\partial}{\partial \theta} [\dot{\theta} F \sin \theta] + \frac{\partial}{\partial \varphi} [\dot{\varphi} F] \tag{2.3}$$

where $\Delta = \frac{1}{\sin \theta} \frac{\partial}{\partial \theta} \left(\sin \theta \frac{\partial}{\partial \theta} \right) + \frac{1}{\sin^2 \theta} \frac{\partial^2}{\partial \varphi^2}$ represents the Laplacian operator.

Seeking for a solution written in term of a series :

$$F = \sum_{j=0}^{\alpha} b^j F_j$$

in which :

$$F_j = \sum_{n=0}^{\infty} \sum_{m=0}^n [a_{n,m,j} \cos (m\varphi) + b_{n,m,j} \sin (m\varphi)] P_n^m$$

we obtain, after substitution of F_j for the series in equation (2.3), three recurrence relations between the $a_{n,m,j}$ and $b_{n,m,j}$. While in the case of Couette flow, the first coefficients could be easily determined once $a_{0,0,0}$ is set to $1/2 \pi$, for the Taylor vortex flow, we shall merely compute the coefficients $a_{n,m,j}$ and $b_{n,m,j}$ which will appear in the final expression of χ and Δn .

2.3 PERMITTIVITY TENSOR OF THE SOLUTION. — This calculation is based on the hypothesis that the electric field of the incident light wave may be treated quasi-statically, this implies that the wavelength is greater than the largest dimension of the particle.

The solution is composed of a suspension of spheroidal particles (permittivity $[\varepsilon]$) bathing in a homogeneous and isotropic medium (permittivity ε_1).

Since the properties, we are measuring (χ and Δn) are macroscopic properties of the liquid, we state that the real discontinuous medium can be idealized by an equivalent continuum of permittivity $[\epsilon']$ [Fig. 9] and write that the polarization of these two equivalent media is equal.

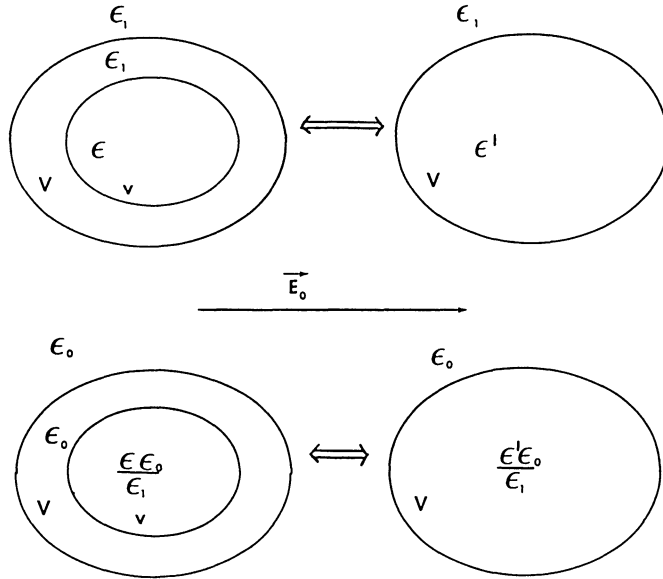


Fig. 9. — Representation of the equivalent dielectric medium.

A simplification arises from the fact that the solution of the polarization problem of a medium of permittivity $[\epsilon]$ placed in a medium of permittivity ϵ_1 is identical to the one of a substance of permittivity $[\epsilon] \epsilon_0/\epsilon_1$ in vacuum [15].

By orientating successively the external influencing field E_0 along the principal directions of polarization of the particle, we obtain the two principal equivalent permittivities ϵ'_\parallel and ϵ'_\perp .

$$\epsilon'_\parallel = \frac{\epsilon_1[\epsilon_1 + (\epsilon_\parallel - \epsilon_1) A_1(0) + \Lambda(\epsilon_\parallel - \epsilon_1)(1 - A'_1(0))]}{\epsilon_1 + (\epsilon_\parallel - \epsilon_1) A_1(0) - \Lambda(\epsilon_\parallel - \epsilon_1) A'_1(0)}$$

$$\epsilon'_\perp = \frac{\epsilon_1[\epsilon_1 + (\epsilon_\perp - \epsilon_1) A_2(0) + \Lambda(\epsilon_\perp - \epsilon_1)(1 - A'_2(0))]}{\epsilon_1 + (\epsilon_\perp - \epsilon_1) A_2(0) - \Lambda(\epsilon_\perp - \epsilon_1) A'_2(0)}$$

where $\Lambda = \frac{v}{V}$ is the volumic concentration of the particles.

The terms $A_\mu(0)$ and $A'_\mu(0)$ represent elliptic integrals the definition of which can be found in reference [16]...

Then in the principal axes of the particle, the permittivity is written as :

$$[\epsilon'] = \begin{vmatrix} \epsilon'_\perp & 0 & 0 \\ 0 & \epsilon'_\perp & 0 \\ 0 & 0 & \epsilon'_\parallel \end{vmatrix}.$$

However it should be noted that the optical properties (χ and the phase angle) are measured referring to a system fixed to the cell and deduced from the principal one by the rotation (θ, φ). Thereby $[\varepsilon']$ should be written in this new coordinates system and becomes $[E]$. Applying Maxwell's equations to the equivalent dielectric medium, we obtain the ellipsoid of the indexes :

$$1 = \varepsilon_0[\Gamma_{xx} x^2 + \Gamma_{yy} y^2 + \Gamma_{zz} z^2 + 2 \Gamma_{xy} xy + 2 \Gamma_{xz} xz + 2 \Gamma_{yz} yz]$$

where the Γ_{ij} are the components of $[E]^{-1}$.

As it could be expected from the fact that the flow presents an axial periodicity, the orientation of the ellipsoid is also dependent in z . This means that the liquid will have to be considered as a superposition of infinitely thin layers the orientation of which varies continuously.

2.4 EXTINCTION ANGLE AND BIREFRINGENCE INTENSITY. — Making use of the results of Leray [17], concerning the composition of small birefringent media and if $\delta(z)$ and $\beta(z)$ represent respectively the phase angle and the azimuth of an infinitely thin layer we can write :

$$\text{tg } 2 \chi = \frac{\int_0^\tau \delta(z) \sin 2 \beta(z) dz}{\int_0^\tau \delta(z) \cos 2 \beta(z) dz}$$

$$\phi^2 = \left[\int_0^\tau \delta(z) \sin 2 \beta(z) dz \right]^2 + \left[\int_0^\tau \delta(z) \cos 2 \beta(z) dz \right]^2$$

where ϕ is the phase angle of the equivalent medium. The Taylor vortex flow being periodical in the axial direction, the integration is performed on a single period τ of the phenomenon.

Introducing the mean components (weighted by the distribution function) of the permittivity tensor we get :

$$\text{tg } 2 \chi = 2 \frac{\int_0^\tau [\langle \varepsilon_{23} \rangle \langle \varepsilon_{13} \rangle - \langle \varepsilon_{12} \rangle \langle \varepsilon_{33} \rangle] / \langle \varepsilon_{33} \rangle dz}{\int_0^\tau [\langle \varepsilon_{33} \rangle (\langle \varepsilon_{22} \rangle - \langle \varepsilon_{11} \rangle) - \langle \varepsilon_{23} \rangle^2 + \langle \varepsilon_{13} \rangle^2] / \langle \varepsilon_{33} \rangle dz}$$

and

$$\Delta n = \frac{1}{2 \tau \varepsilon_0 n_m} \left[\left[\int_0^\tau \frac{2(\langle \varepsilon_{13} \rangle \langle \varepsilon_{23} \rangle - \langle \varepsilon_{12} \rangle \langle \varepsilon_{33} \rangle)}{\langle \varepsilon_{33} \rangle} dz \right]^2 + \left[\int_0^\tau \frac{\langle \varepsilon_{33} \rangle [\langle \varepsilon_{22} - \langle \varepsilon_{11} \rangle]}{\langle \varepsilon_{33} \rangle} + \langle \varepsilon_{13} \rangle^2 - \langle \varepsilon_{23} \rangle^2 dz \right]^2 \right]^{1/2}$$

n_m the average index and

$$\langle \varepsilon_{ij} \rangle = \frac{1}{4 \pi} \int \varepsilon_{ij} F(\theta, \varphi) \sin \theta d\theta d\varphi$$

where

$$\begin{aligned}\langle \varepsilon_{13} \rangle &= -\frac{2\pi}{5} (\varepsilon'_\perp - \varepsilon'_\parallel) \sum_j b^j a_{2,1,j} \\ \langle \varepsilon_{23} \rangle &= -\frac{2\pi}{5} (\varepsilon'_\perp - \varepsilon'_\parallel) \sum_j b^j b_{2,1,j} \\ \langle \varepsilon_{12} \rangle &= -\frac{8\pi}{5} (\varepsilon'_\perp - \varepsilon'_\parallel) \sum_j b^j a_{2,2,1} \\ \langle \varepsilon_{33} \rangle &= \varepsilon'_\parallel + \frac{1}{3} (\varepsilon'_\perp - \varepsilon'_\parallel) + \frac{8\pi}{15} (\varepsilon'_\perp - \varepsilon'_\parallel) \sum_j b^j a_{2,0,j} \\ \langle \varepsilon_{22} \rangle - \langle \varepsilon_{11} \rangle &= -\frac{16\pi}{5} (\varepsilon'_\perp - \varepsilon'_\parallel) \sum_j b^j a_{2,2,j}.\end{aligned}$$

The birefringence intensity of the solutions is weak ; thus the difference $\varepsilon'_\perp - \varepsilon'_\parallel$ is small compared to either one or the other of the permittivities : a factor such that $\langle \varepsilon_{33} \rangle$ equals nearly ε'_\parallel . On the other hand, the solutions are highly diluted so that Λ is also very small. These considerations allow us to assume :

$$\frac{\langle \varepsilon_{23} \rangle \langle \varepsilon_{13} \rangle}{\langle \varepsilon_{33} \rangle} \ll \langle \varepsilon_{12} \rangle$$

and

$$\langle \varepsilon_{22} \rangle - \langle \varepsilon_{11} \rangle < \langle \varepsilon_{23} \rangle^2 \quad \text{or} \quad \langle \varepsilon_{13} \rangle^2.$$

Finally, the angle of extinction and the birefringence intensity can be expressed as :

$$\text{tg } 2\chi = \frac{\int_0^\tau \sum b^j b_{2,2,j} dz}{\int_0^\tau \sum b^j a_{2,2,j} dz}$$

and

$$\Delta n = \text{cste} \left[\left[\int_0^\tau \sum b^j b_{2,2,j} dz \right]^2 + \left[\int_0^\tau \sum b^j a_{2,2,j} dz \right]^2 \right]^{1/2}$$

with

$$\text{cste} = \frac{1}{2\tau\varepsilon_0 n_m} \left[\frac{16\pi}{5} \right] (\varepsilon'_\perp - \varepsilon'_\parallel).$$

For later use, the term in brackets in the expression of Δn shall be called $F(\sigma, b)$, ($\sigma = \frac{G}{d}$).

We note that in the frame of the approximations, the results for $\text{tg } 2\chi$ and Δn are not very different from the classical ones ; as a matter of fact in this case, the previous relations are :

$$\text{tg } 2\chi = -\frac{2\langle \varepsilon_{12} \rangle}{\langle \varepsilon_{22} \rangle - \langle \varepsilon_{11} \rangle} = -\frac{\sum_j b^j b_{2,2,j}}{\sum_j b^j a_{2,2,j}}$$

$$\Delta n = \frac{1}{2 \varepsilon_0 n_m} [4 \langle \varepsilon_{12} \rangle^2 + (\langle \varepsilon_{22} \rangle - \langle \varepsilon_{11} \rangle)^2]^2$$

$$\Delta n = \frac{1}{2 \varepsilon_0 n_m} (\varepsilon_{\perp} - \varepsilon_{\parallel}) \left[\left(\sum_j b^j b_{2,2,j} \right)^2 + \left(\sum_j b^j a_{2,2,j} \right)^2 \right].$$

The complexity of the previous expressions $\text{tg } 2\chi$ and Δn does not allow for the prospect of finding a simple analytical form easy to handle like in the case of the classical Couette flow.

Thus, we have performed a numerical calculation of the angle χ and of the birefringence Δn beyond the critical value T_c . The only adjustable parameter (scaling factor f) remaining in the equations (arising from the fact that the tangential velocity component is a solution of an homogeneous system) is chosen to obtain the best agreement with our experiments.

3. Experimental part.

Experimental measurements have been performed on aqueous solutions of flattened particles like bentonite and rod-like particles like T.M.V. The details of these studies are found in reference [3]. The optical properties are measured by the classical method of Senarmont. When submitted to a shear flow, the liquid containing rigid anisodiametrical particles becomes birefringent and two characteristic quantities can be measured : the extinction angle χ defined as the angle between a neutral line and the direction of the flow and the phase angle φ related to the birefringence intensity Δn by the relation :

$$\varphi = \frac{2\pi}{\lambda} \Delta n.$$

3.1 OPTICAL DEVICE. — The ellipsometer used in the experiments is composed (see Fig. 10) of two polarizing devices P_1 and P_2 which remain crossed during the determination of the position of the neutral lines of the liquid under flow. A quarter wave plate $\lambda/4$ can be introduced in the light path in order to measure the phase angle φ of the medium.

3.2 COUETTE CELL. — The classical Couette cell is built from two coaxial glass cylinders fitted together and making up an annular space in which a thermostatic liquid can flow. The manufacture of the inner one has received special care and the inner radius of the cylinder is constant within ± 0.01 mm all along its length. Inner rotating cylinders of various radii are made of stainless steel. The typical dimensions of the cell are :

diameter of outer cylinder	: 50 mm
diameter of inner cylinders	: 46, 47, 48 mm
height of the cell	: 70 mm

3.3 SOLUTIONS OF RIGID PARTICLES. — Two kinds of rigid particles, different by their shape, have been used in aqueous solutions : bentonite, a clay material and Tobacco mosaic virus (T.V.M). The particle of bentonite appears like a leaf of a 100 to 200 Å in thickness and up to 10 000 Å in length while the particle of T.M.V. looks like a rod of 3 000 Å in length and 150 Å in diameter.

Preparation of the solution.

A definite amount of dry material (2 g) is poured in distilled water and the mixture is shaken mechanically for several hours. After decanting, the remaining liquid undergoes several

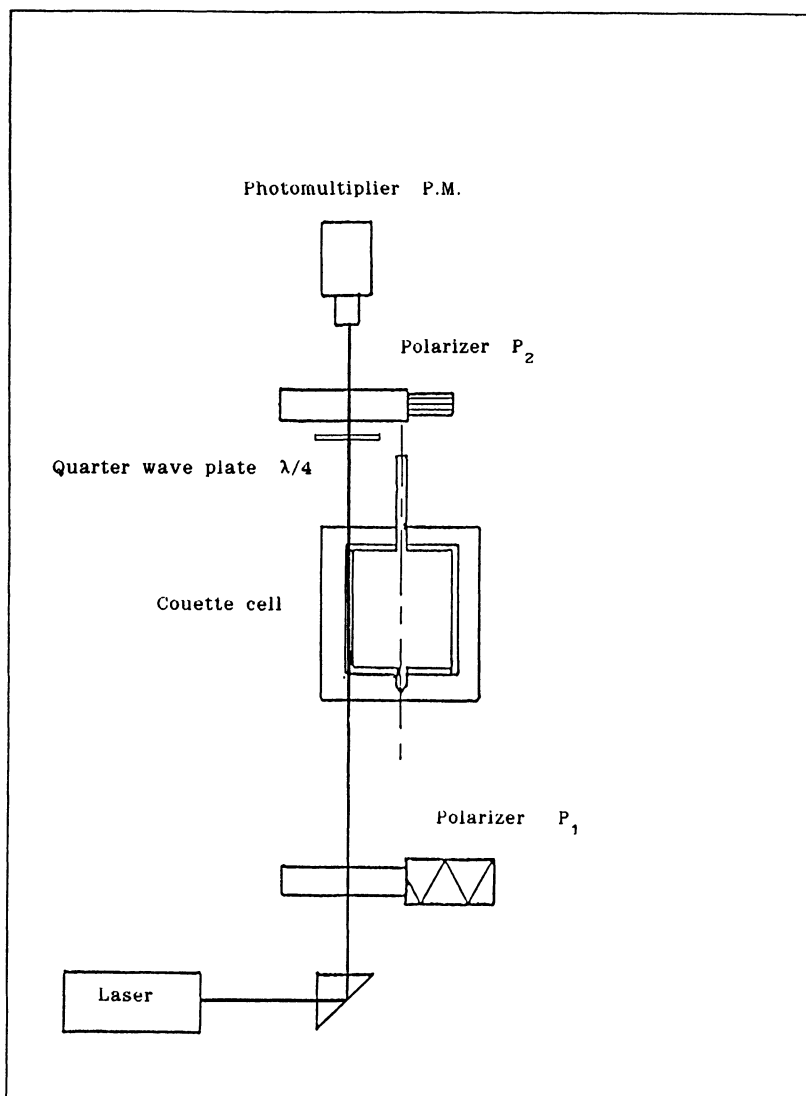


Fig. 10. — Schematic representation of the ellipsometer.

filtrations, the last one being made on a Micropore filter of 0.45μ . Finally and just before use, the solution is submitted to centrifugation at 10 000 rvs/min during 20 minutes.

The sample of purified T.M.V. has been offered to us by Professor Jean Vitz of the Botanical Institut of Strasbourg. The initial concentration of 34 mg/ml is reduced to 1 mg/ml by addition of a phosphate buffer.

4. Comparison with experiments. Discussion.

4.1 BENTONITE. — The experimental results referring to this type of particle are reported in the curves shown in figures 11a and 11b. The study has been performed for two widths of the

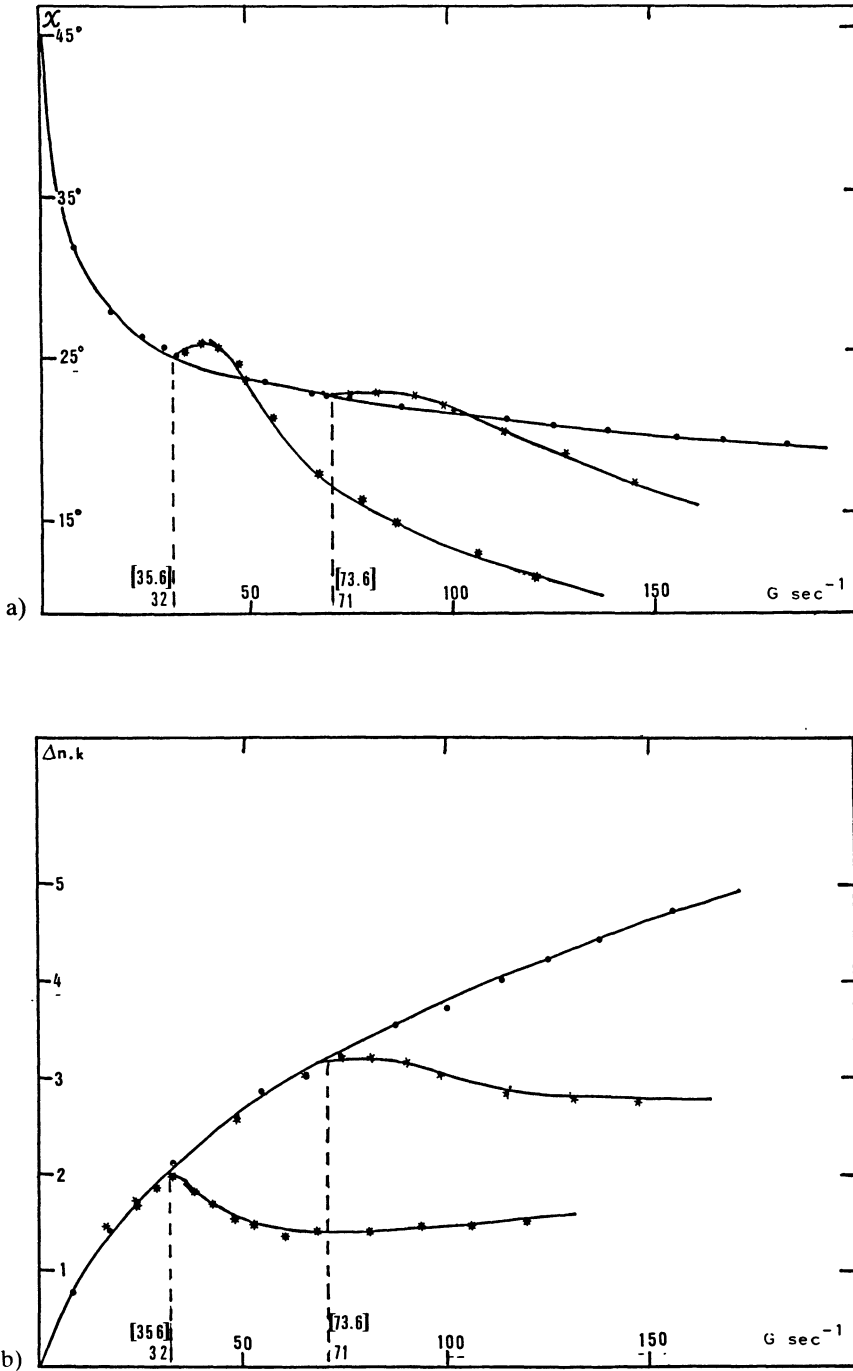


Fig. 11. — (a) Variation of the extinction angle χ versus G for different widths of the annular gap (case of bentonite solution). 1 mm (●), 1.5 mm (★), 2 mm (*) (in brackets, above the experimental values, the corresponding critical gradient computed from the expression of T). (b) Variation of the birefringence intensity for different widths of the annular gap (case of bentonite solution). 1 mm (●), 1.5 mm (★), 2 mm (*), $k = 2.04 \times 10^7$ (in brackets, above the experimental values, the corresponding critical gradient computed from the expression of T).

annular gap (1.5 mm and 2 mm). As the gradient G increases and finally reaches the critical value G_c corresponding to T_c , the angle χ increases first to a maximum and then falls rapidly towards the direction of the flow. This maximum exists also in the case of 1.5 mm gap, but appears to be less sharp.

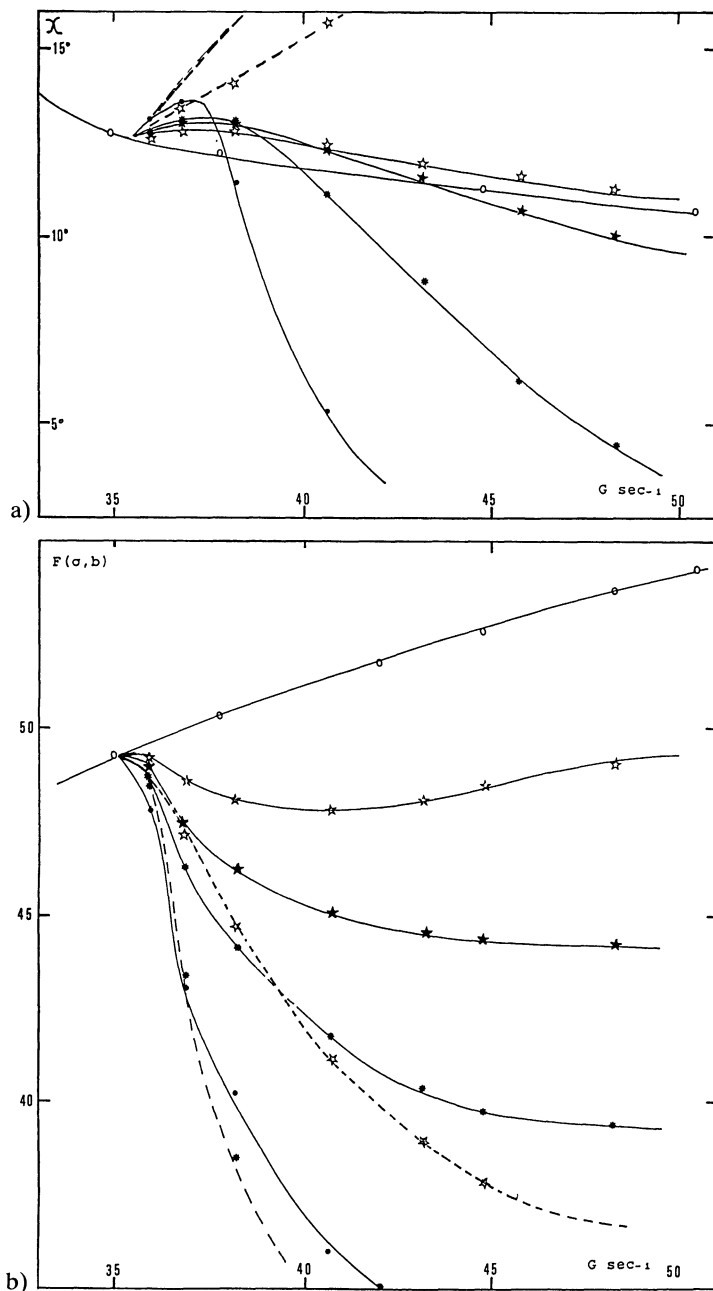


Fig. 12. — (a) Theoretical variation of χ versus G for different scaling factors in the case of a bentonite solution. 0.03 (\star), 0.04 (\blackstar), 0.05 ($*$), 0.07 (\bullet) (theoretical value of G_c : 35.6 s^{-1}). (b) Theoretical variation of Δn versus G for different scaling factors in the case of a bentonite solution. 0.03 (\star), 0.04 (\blackstar), 0.05 ($*$), 0.07 (\bullet) (theoretical value of G_c : 35.6 s^{-1}).

Looking at the birefringence (Fig. 11b), we note, as G reaches the critical value G_c , a disastrous drop of Δn in comparison with the value we would measure in the case of Couette flow for the same value of G .

The corresponding theoretical results obtained in the case $b = -1$, are presented in the figures 12a and 12b. A surprisingly good qualitative agreement is obtained when we choose a scaling factor around 0.05 in the case $a < a_c$ (plain lines).

The same conclusion can be drawn with the curves $F(\sigma, b)$. If we choose $a > a_c$ the computation of χ and $F(\sigma, b)$ leads to the results represented by broken lines : the only satisfactory result is obtained for the curve $F(\sigma, b)$ when the scaling factor f equals 0.05 ; a complete disagreement between theory and experiment can be noticed in the case of the angle χ which is seen to increase continuously when $G > G_c$.

4.2 TOBACCO MOSAIC VIRUS. — These results are reported in figures 13a and 13b for the experiments and 14a and 14b for the theoretical calculations.

Starting in the Couette flow region, we gradually increase G and by reaching G_c , the same break in the curve $\chi(G)$ and $\Delta n(G)$ appears ; although the extinction angle χ shows a flattened plateau instead of a maximum with this kind of particle. The same sharp break is observed with the birefringence intensity for $G = G_c$.

The results of our computation show a fairly good agreement for the variation of χ versus G in the case $a > a_c$ (plain line in Fig. 14a) : the curves do not show a maximum as in the case of bentonite solution for any scaling factor f .

The case $a < a_c$ is represented by the broken lines : the results are not basically different from the case $a > a_c$ but the evolution of $F(\sigma, b)$ versus G (Fig. 14b) shows clearly that the only satisfactory case corresponds to $a > a_c$: as a matter of fact we note that, for all f , $F(\sigma, b)$ is very close to the corresponding curve of the Couette flow for all G .

5. Conclusion.

The emergence of a periodic flow in a Couette cell when the angular velocity of the rotating cylinder is gradually increased will have an important effect in the dynamo-optical properties of the solution.

This fact can indeed be easily admitted if we know that these properties depend on the degree of orientation of the particles which in turn, depends heavily on the structure of the hydrodynamical field.

The experimental measurements of these properties should also show, in some manner, the emergence of this second flow superimposed to the underlying laminar Couette flow : the measurements of the induced birefringence in the range where this transition happens confirm this fact.

The breaks observed in the birefringence intensity curves $\Delta n(G)$ are sharp enough to determine quite accurately the critical gradient at which the transition appears : thus the birefringence intensity measurements appears to be an interesting method in the determination of the emergence of the vortices and can be compared to the torque measurements method [18].

In addition, it seems that the shape of the particle in the liquid plays an important part in the manner in which these properties behave when G is still increased after G_c : unlike the curves $\chi(G)$ and $\Delta n(G)$ corresponding to the Couette flow and which show the same qualitative aspect whatever the shape of the particle may be, the variation of the angle of extinction χ in the Taylor flow is greatly affected by the shape of the particle in solution and thus, its study gives us the means of distinguishing between the flattened and elongated particle.

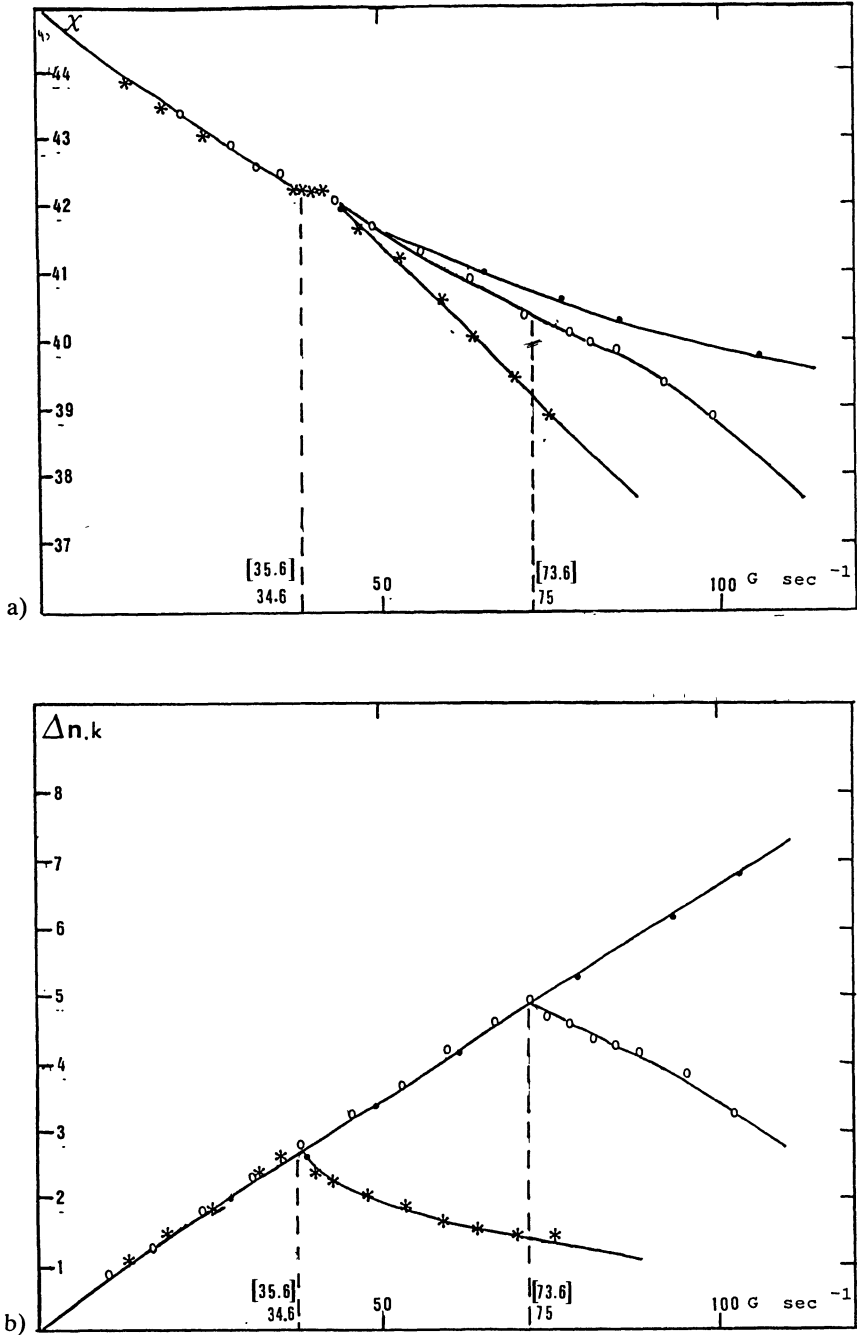


Fig. 13. — (a) Variation of the extinction angle χ versus G for different widths of the annular gap (case of T.M.V. solution). 1 mm (●), 1.5 mm (○), 2 mm (*) (in brackets, above the experimental values, the corresponding critical gradient computed from the expression of T). (b) Variation of the birefringence intensity for different widths of the annular gap (case of T.M.V. solution). 1 mm (●), 1.5 mm (○), 2 mm (*), $k = 2.04 \times 10^7$ (in brackets, above the experimental values, the corresponding critical gradient computed from the expression of T).

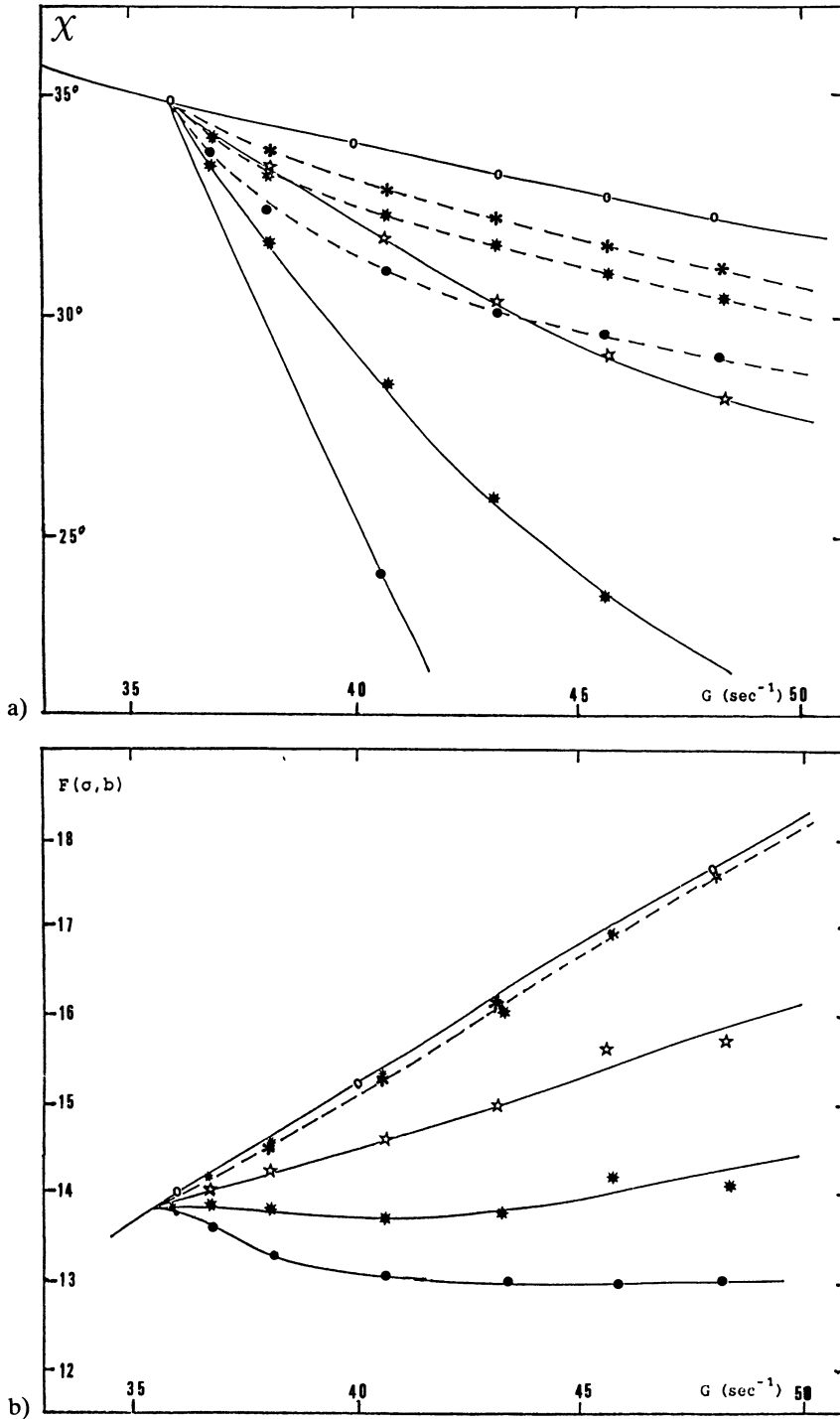


Fig. 14. — (a) Theoretical variation of χ versus G for different scaling factors in the case of a T.M.V. solution. 0.03 (☆), 0.04 (*), 0.05 (*), 0.07 (●) (theoretical value of G_c : 35.6 s^{-1}). (b) Theoretical variation of Δn versus G for different scaling factors in the case of a T.M.V. solution. 0.03 (☆), 0.04 (*), 0.05 (*), 0.07 (●) (theoretical value of G_c : 35.6 s^{-1}).

These experimental conclusions are confirmed by the theoretical computation of these same properties.

The critical Taylor number T_c corresponding to the first transition from Couette flow to Taylor vortex flow is in total agreement with the value proposed by different authors as shown in table I.

Our calculation is based on the resolution of a system of linearized equations which are valid only in the region of gradients slightly above the critical gradient G_c and if the flow remains in its axisymmetric form. However we have assumed that the velocity components derived from it could be used in an extended region to compute χ and $F(\sigma, b)$ for the values of G well above G_c . We know also from visual observation and different authors [19, 20], that a wavy flow in the axial direction superimposes to the first Taylor flow rather quickly in the case of a narrow gap which represents our case. But when we compare the theoretical results with the experimental curves of $\chi(G)$ and $\Delta n(G)$, the agreement is complete in all the range of variation of G .

This conclusion tends to prove that the azimuthal wave has little influence on the optical properties measured in the axial direction.

Another interesting conclusion of this work is that, at least theoretically, it appears possible to reach the intrinsic permittivities ε_{\perp} and ε_{\parallel} of the particle by associating the results obtained in the case of Couette and Taylor flows: the slope at the origin of the curve $\Delta n(G)$ in the Couette flow leads to the difference $\varepsilon_{\perp} - \varepsilon_{\parallel}$ while, in the case of Taylor flow, we can reach one of the permittivities ε_{\parallel} .

References

- [1] TAYLOR G. I., *Trans. Roy. Soc. London A* **223** (1923) 289.
- [2] WAYLAND H., *J. Appl. Phys.* **26** (1955) 1197.
- [3] DECRUPPE J. P., Thèse d'Etat, soutenue le 1^{er} juillet 1988.
- [4] HALLER W., *Kolloid-Z.* **61** (1932) 26.
- [5] BOEDER P., *Z. Phys. Chem.* **75** (1932) 258.
- [6] KUHN W., *Z. Phys. Chem.* **161A** (1932) 1,427.
- [7] SADRON C., *J. Phys. Rad.* **8** (1937) 481.
- [8] PETERLIN A. and STUART H. A., *Z. Phys.* **112** (1939) 1,129.
- [9] PERRIN F., *J. Phys. Rad.* **5** (1934) 33.
- [10] CHANDRASEKHAR S., *Hydrodynamic and Hydromagnetic Stability* (Oxford Univ. Press.) 1961.
- [11] DIPRIMA R. C., *Quart. Appl. Math.* **18** (1961) 375.
- [12] NSOM EYENGA NDILLE B., Thèse de l'Université de Metz (1987).
- [13] DAVEY A., *J. Fluid. Mech.* **14** (1962) 336.
- [14] JEFFERY G. B., *Proc. Roy. Soc. London A* **120** (1922) 161.
- [15] LANDAU L. and LIFCHITZ E., *Electrodynamique des milieux continus* (1969).
- [16] DURAND E., *Electrostatique III. Méthodes de Calcul Diélectriques* (Ed. Masson) 1968, p. 242.
- [17] LERAY J. and SCHEIBLING G., *J. Chim. Phys.* (1961) 797.
- [18] COLE J. A., *J. Fluid. Mech.* **75** (1976) 1.
- [19] DAVEY A., DIPRIMA R. C. and STUART J. T., *J. Fluid. Mech.* **31** (1968) 17.
- [20] EAGLES P. M., *J. Fluid. Mech.* **49** (1971) 529.
- [21] KRUEGER E. R., GROSS A. and DIPRIMA R. C., *J. Fluid. Mech.* **24** (1966) 521-538.
- [22] EAGLES P. M., *J. Fluid. Mech.* **49** (1971) 529-550.